Iranian Journal of Mechanical Engineering
The Iranian Society of Mechanical Engineers
Research Paper

DOI: 10.30506/JMEE.2021.529536.1259

S. Karimi[*]
Assistant Professor

A. Abiri[†]
Researcher

M. Shafiee[‡]
Assistant Professor

H. Abbasi[§]
Assistant Professor

F. Ghadam[**]
Researcher

New Correlations for the Prediction of Terminal Velocity and Drag Coefficient of a Bubble Rising

The present experimental study was done aimed to investigate dynamic of a single bubble rising through wall-bounded flow at high Reynolds number. Thus, Rhamnolipid biosurfactant was added to stagnant fluid and bubble diameter was controlled between 2.5 and 3.5mm. The resulted Reynolds number was in the range of 400 to 900 depends on biosurfactant concentration. Rhamnolipid has a low toxicity, a high biodegradability and good stability at a wide range of temperatures. The results showed that terminal velocity linearly depends on Reynolds number. Furthermore, drag coefficient is related to Eötvos number and is autonomous to Reynolds number. Finally, to estimate terminal velocity and drag coefficient, four empirical correlations were developed. Relative errors of the proposed correlations were less than of 3.35% and 1.97% for velocity and dimensionless velocity equations, respectively, and average errors of two equations proposed for drag coefficient were 4.44% and 3.26%.

Keywords: High Reynolds number, Rhamnolipid biosurfactant, Terminal velocity, Drag coefficient, Wall-bounded flow.

1 Introduction

Two-phase flow is a common phenomenon in essential processes of industries such as chemical, food, petro-chemical and biochemical refinery processes. One of the challenges here is predicting flow behavior in bubbly flows, where the bubbles flow through a continuous fluid phase. According to the researches, the flow pattern is controlled by the liquid and gas properties such as viscosity, density, surface tension, difference of density between phases, solute concentration, bubble diameter and rising velocity [1-4] However, the phenomenon is not completely known, particularly for large bubble at wall-bounded flow. Single bubble shape and its terminal velocity change depend on kind of flow regime.

[*] Corresponding Author, Assistant Professor, Chemical Engineering Department, Jundi-Shapur University of Technology, Dezful, Iran, s.karimi@jsu.ac.ir

[†] Researcher, Chemical Engineering Department, Jundi-Shapur University of Technology, Dezful, Iran, ana.abiri1991@gmail.com

[‡] Assistant Professor, Chemical Engineering Department, Jundi-Shapur University of Technology, Dezful, Iran, shafiee@jsu.ac.ir

[§] Assistant Professor, Chemical Engineering Department, Jundi-Shapur University of Technology, Dezful, Iran, habbasi@jsu.ac.ir

[**] Researcher, Mechanical Engineering Department, Jundi-Shapur University of Technology, Dezful, Iran, farzad.ghadam7584@gmail.com

Receive: 2021/05/03 Accepted: 2021/09/12

Based on the dominant force, there are three regimes: 1) viscosity region, 2) intermediate region (surface tension, viscous and inertia forces), and 3) inertia region. It is established that Reynolds number is a key parameter in individualizing these regimes which is affected on rising terminal velocity and the drag coefficient of bubbles [5]. This means that the velocity greatly relates to Reynolds number when it is low, whereas this dependency decreases at high Reynolds number [6]. Most studies examined the motion of bubble in the intermediate region [7-9]. Moor [10] proposed an equation for drag force of a small bubble in this regime. Lehrer [11] suggested an equation of terminal velocity for large bubble in both intermediate and high Reynolds number where inertia and surface tension forces are significant. Almatroushi and Borhan [12] measured terminal velocities of Taylor bubble in glycerol–water solutions contaminated with SDS surfactant at low Reynolds numbers and denoted that the presence of surfactant increases terminal velocity. Liu et al. [13] stated, the bubbles stay almost spherical in the viscous-dominated regime and their surface of the bubble remain almost stable. Zhang et al. [14] reported that the bubble velocity is independent on bubble diameter in the range between 2*mm* and 5*mm*, in the surface tension dominant regime. However, few work is done on the behavior of large bubbles at high Reynolds number, inertia region [15-20].

Bozzano and Dente [21] evaluated the interaction between bubble velocity and its shape in high Reynolds number. They concluded that the velocity greatly affected the shape of the bubble. Similar results were also obtained by Liu et al.[13]. Riboux et al. [22] also investigated hydrodynamics of a bubble-induced agitation and showed that at high Reynolds number it is independent of bubble diameter. In another study Yan et al. [23] experimentally studied bubble velocity in water and showed that the terminal velocity periodically fluctuates with different height. Recently, Tihon and Eeji [24] considered the velocity of large bubble rising within vertical columns of liquid in the inertia flow regime and concluded that the terminal velocity is related to square root of the channel perimeter. Generally, studies show that for large single bubbles, there is a competition between inertia and surface tension, while for small bubbles, it can be negligible [25, 26]. Nevertheless, more researches are needed to realize the bubble behavior in this regime. In order to obtain a precise prediction of bubble hydrodynamics, various studies focus on drag force, believed that it is the most important force in regulating bubble motion [27-31]. Deng et al. [32] described the variation of drag coefficient with the bubble size ranging from microns to millimeters according to the interfacial tension, internal circulation and shape deformation without considering the effects of the wall. It can be seen at low Reynolds; the drag coefficient depends on the Reynolds number [33-38]. However, at high Reynolds number the bubble behaves differently [14, 20, 39, 40]. So far, many drag coefficient correlations reported for the bubble rising at low Reynolds number [41-46]. While less study could found to investigate motion of large bubble at high Reynolds number. In addition, studies show that wall plays an important role in the bubble motion within the liquid [47-49]. Analyzing wall effects on bubbles and drops is more difficult than quantifying it for rigid particles [50]. Hence, very few studies have carried out on wall effects. Most studies used the influence of the diameter ratio (ratio of equivalent diameter to column diameter) on the terminal velocity to determine wall effects [51-53]. The effects of wall on the motion of rigid particles in non-Newtonian fluids is considered by Chhabra [50].

Also, Clift et al. [51] studied effects of wall at low Reynolds number and show the velocity decreases with increasing the bubble diameter ratio. Based on our knowledge, there is no study to examine the behavior of bubble in narrow channel at high Reynolds number. Therefore, in this study, the velocity and drag coefficient of a single large bubble rising in wall-bounded flow at high Reynolds number were investigated. To increase Reynolds number, biosurfactant was added to the liquid phase resulting viscosity reduction. Its drag coefficient and terminal velocity were calculated by experimental measurements and new correlations were presented to predict

them by curve fitting method. The results of the study were compared with various experimental studies, to confirm the validity of the present study results.

2 Materials and methods

2.1 Experimental set-up

Figure (1) schematically presents the experimental apparatus. It includes a vertical Plexiglass column filled with biosurfactant-contaminated water that is continues phase in this work. The dimensions of column are $450mm \times 40mm \times 40mm$ with thickness of $5mm$. The study zone was high enough, $175mm$ above the column floor, to ensure that the recorded velocity is bubble terminal velocity. Tests were repeated at least three times for each case and averaged between the results. The column size was selected so that the bubble rising is limited by the walls called wall-bounded flow [47, 54, 55]. The column was open to atmosphere and the experiments were carried out at ambient temperature ($19^{\circ}C$). Single bubble was injected through different needle to control its diameter. The internal diameter of needles consists of 0.7,0.9,1.2 *and* 1.6*mm*. In order to supply the air, a flexible tube was used connecting the needle to syringe pump. The gas flow rate was fixed to $0.4ml/\min$. It was so low that the bubble shape was determined by balance between the buoyancy and the surface tension forces. Moreover, this low flow rate was chosen to prevent the bubbles interaction, practically.

The bubble trajectory was monitored and recorded by a camera. A 100*mm* macro lens (AT-X M100 Pro, Tokina, Japan) was used to obtain high-resolution images of the bubbles. Lighting balance is very important in these experiments. Thus, a LED lamp was embedded at adequate location of the column. In addition, a semitransparent diffuser was located between them to delete the reflection from the bubble surface. In order to increase Reynolds number, liquid phase viscosity was reduced by adding biosurfactant. The selected biosurfactant for this purpose was rhamnolipid, which has been described previously by the others [47, 56].

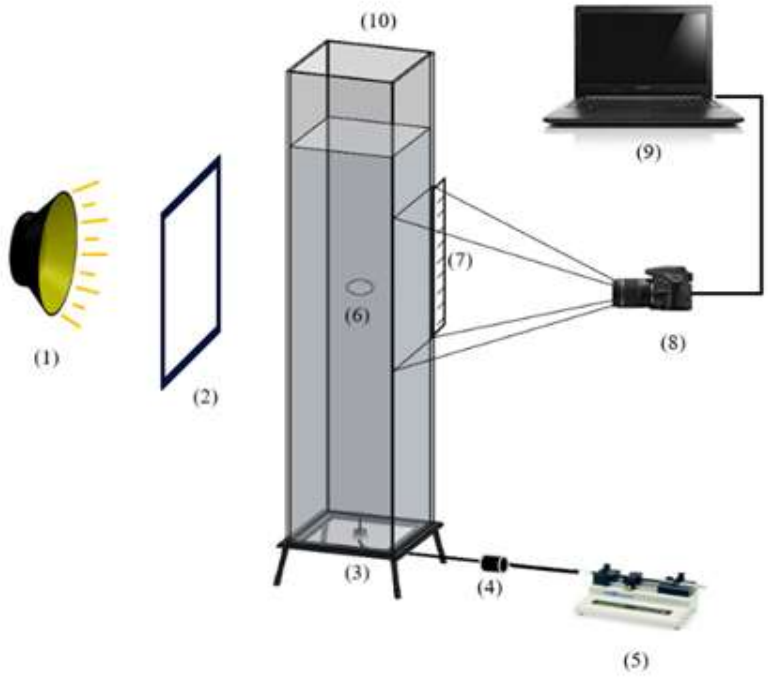

Figure 1 Schematic of experimental apparatus, 1: LED lamp, 2: Diffuser, 3: Needle, 4: One -way valve, 5: Syringe pump, 6: Bubble rising in the liquid column, 7: Ruler, 8: Camera and macro lens, 9: Image processing system, 10: Liquid column.

2.2 Image Processing

The camera monitored bubble trajectory via recording a video. The video was converted to a collection of images. Bubble location and its geometric parameters were obtained by analyzing this collection, using image processing. Its steps were described by the authors previously [47].

2.3 Drag coefficient calculation

The Main forces acting on a rising bubble with constant velocity through a stationary fluid, are buoyancy, drag, and weight force. While these forces are in balance, the drag coefficient can be calculated as follows:

$$C_D = \frac{4d_{eq}g}{3U_t^{\,2}} \tag{1}$$

where U_t is terminal velocity and g is the gravitational acceleration. Equivalent diameter of bubble, d_{eq}, was calculated according to its area square root ($d_{eq} = \sqrt{4A_b/\pi}$), where $A_b(mm^2)$ is bubble area.

Early studies show that drag coefficient mostly relates to Reynolds $\left(\mathrm{Re} = \rho_L d_{eq} U_t / \mu_L\right)$, Archimedes ($Ar = \rho_L^2 g d_{eq}^3 / \mu_L^2$) and Eötvös $\left(Eo = \Delta\rho g d_{eq}^2 / \sigma\right)$ numbers. The Eötvös number, measures the importance of gravitational and surface tension forces relative to each other. Moreover it used together with Morton number ($Mo = g\mu_L^{\,4}(\rho_L - \rho_g) / \rho_L^2\sigma^3$) or Archimedes to describe the bubble or droplet shape moving within stagnant liquid.

3 Results and Discussion

In the present study, the experiments were carried out with four different needles diameter by injecting air in a biosurfactant-contaminated fluid. The bubble equivalent diameter was between 2.5-3.5*mm*, depends on the size of the needles. It is demonstrate by Tomiayama et al., [39] that bubbles of 1.3 *mm* to 6 *mm* are intermediate bubble in which both surface tension and inertia force effects are significant. The selected biosurfactant was rhamnolipid. According to our knowledge, it is a good choice to provide high Reynolds condition. Table (1) shows important physical parameters of the experiments at different biosurfactant concentration. According to table 1, the more surfactant concentration, the less solution viscosity. Whereas below critical micelle concentration (CMC), surface tension decrease, then it becomes constant. However, the density does not depend to the concentration. The resulted three dimensionless numbers are tabulated in Table (2). In the fallowing, the effect of these dimensionless numbers on the drag coefficient and velocity is investigated.

Table 1 Physical parameters for different solution concentration

concentration (***ppm***)	**μ** (***cp***)	**σ** (***N/m***)	**ρ** (***kg/m³***)
10	0.967	0.03925	1000
20	0.933	0.02833	1000
30	0.900	0.027735	1000
40	0.867	0.027735	1000
50	0.833	0.027735	1000

3.1 Bubble terminal velocity

Figure (2) shows the bubble terminal velocity versus its equivalent diameter. Its calculation procedure has already been explained in some detail by Karimi et al. [47]. According to Figure (2), terminal velocity almost tends to increase by increasing equivalent diameter. The increase was not too significant, so that the terminal velocity was in the range of 180 *mm/s* and 205 *mm/s* for bubble equivalent diameters of 2.5–3.5 *mm*. Li et al. [6] showed that terminal velocity first increases dramatically with equivalent diameter, then the increase becomes less noticeable when the equivalent diameter exceeds 2 *mm*. According to the diameter range of the present study, the obtained results were in agreement with Li et al. [6]. Moreover, the results are accordance to the finding of Mahmoudi et al. [57] obtained for air-kerosene system. This agreement was expected, due to the same range of the surface tension of the both studies.
Recently, the bubble terminal velocity in three different surfactant aqueous solutions (MIBC, OP-10, and 2-octanol) was investigated by Zhang et al. [54]. In their study, the wall effects were neglected. They showed that the more equivalent diameter, the more terminal velocity. Their bubble equivalent diameter is in the range of 1.5 *mm*–5 *mm*, and the resulted terminal velocity varies from 160 *mm/s* to 230 *mm/s*. These ranges are in good agreement with the results of the presents experiments. Ziqi et al. [58] and Tomiyama et al. [39] also shown that the terminal velocity increases by increasing diameter. The bubble terminal velocity reported by Tomiyama et al. [39] for diameter range of the present work is 180 to 210 *mm/s* within distillated water. The range is similar to the results of our work done in biosurfactant-contaminated water. However, it is expected that the presence of impurities influences bubble internal circulation and results in a decrease in bubble velocity [32]. The authors attribute this contradiction to being wall-bounded flow in the present study. Because the wall-bounded flow is less affected by the present surfactant [47, 54]. Considering the simple correlation provided by Harmathy [59], bubble terminal velocity is independent of bubble diameter. The correlation is represented to calculate terminal velocity of large bubbles in turbulent region.

Table 2 The resulted dimensionless numbers for different solution concentration

diameter of needle (*mm*)	concentration (*ppm*)	*de* (*mm*)	*Re*	*Eo*	$Mo\times 10^{10}$
0.7	10	2.728	675.4	1.857	1.416
	20	2.561	633.4	2.267	3.268
	30	2.871	703.1	2.911	3.012
	40	2.569	690.1	2.331	2.594
	50	2.621	715.0	2.426	2.213
0.9	10	3.418	699.8	2.915	1.416
	20	3.135	658.6	3.397	3.269
	30	3.403	747.1	4.089	3.012
	40	3.213	732.7	3.647	2.594
	50	3.203	761.9	3.624	2.213
1.2	10	3.436	687.1	2.945	1.416
	20	2.686	567.3	2.494	3.268
	30	3.349	757.6	3.961	3.012
	40	2.669	624.5	2.515	2.594
	50	3.637	896.1	4.672	2.213
1.6	10	3.388	690.5	2.864	1.416
	20	2.782	581.7	2.676	3.269
	30	3.489	778.5	4.299	3.012
	40	3.261	749.4	3.756	2.594
	50	3.193	761.2	3.601	2.213

The Harmathy [59] empirical correlation is defined as follows:

$$U_t = 1.53\left(\frac{g\sigma}{\rho_L}\right)^{0.25} \tag{2}$$

where σ is the liquid surface.

Recently, for free bubble rising through a contaminated fluid with rhamnolipid, a similar empirical correlation proposed by Karimi et al. [47]. They also not considered the bubble diameter. Their correlation is expressed as:

$$U_t = 332\left(\frac{g\sigma}{\rho_l}\right)^{0.07} \tag{3}$$

Figure (2) compares the terminal velocities predicted by Haramthy [59] and Karimi et al. [47] equations and the obtained results. As shown, the obtained velocity is within the range, but the correlations (Eqs. (2) and (3)) do not exhibit the increasing trend. It is noted, in these correlations, the surface tension of the solutions with the concentration above the CMC, which is constant, was used to calculate terminal velocity.

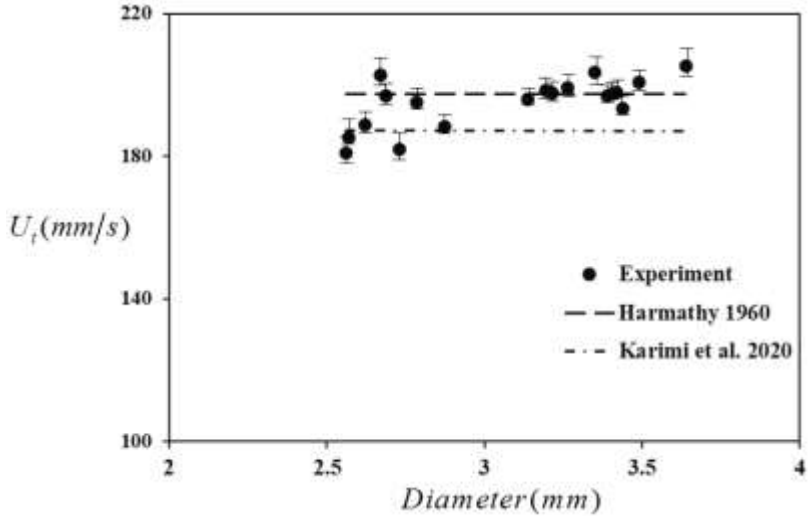

Figure 2 Bubble terminal velocity versus its diameters; a comparison with Harmathy (1960) and Karimi et al. (2020) equations

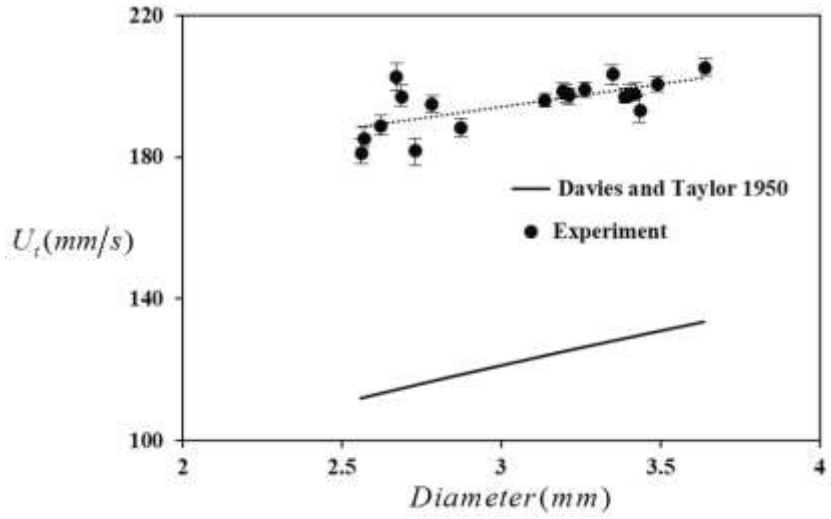

Figure 3 Bubble terminal velocity versus diameter; a comparison with Daveis and Taylor correlation

Davies and Taylor [60] provided a correlation for large bubble rise through nitrobenzene or water in which the velocity dependency to equivalent diameter was taken into account as follows:

$$U_t = 0.707\sqrt{gd_{eq}} \tag{4}$$

Figure (3) compares the terminal velocities predicted by Davis and Taylor [60] equation and the obtained results.

The main reasons for the discrepancy of the present results with Davis and Taylor [60] results are: 1) Reynolds number ranges of two studies are different ($2700 \le \mathrm{Re} \le 8700$ in Davis and Taylor results); 2) the present work was done in wall-bounded flow. According to Figure (3) for the present conditions (rhamnolipid solutions in the wall-bounded flow) a relation between terminal velocity and equivalent diameter can be provided as same as Davies and Taylor [60] correlation with adjusted coefficient. It was obtained by curve fitting method as below:

$$U_t = 1.13\sqrt{gd_{eq}} \qquad (2.5mm < d_{eq} < 3.7mm) \tag{5}$$

The average error between the evaluated equation and experimental data is about 3.35%. It is noted, Eq. (5) is valid only for the range of $400 \le \mathrm{Re} \le 900$ in wall-bounded flow.

Vecer et al. [61] studied the effect of bubble diameter on rising velocity of bubble in three different regions called viscous, surface tension and inertia regions. These ranges strongly depend on bubble size and liquid bulk properties. They presented a new correlation for characteristic bubble size scaled by the effect of viscosity and bubble shape for Reynolds number ranged from 60 to 2200. Vecer et al. [61] empirical correlation is:

$$V_d = 1.2D_d^{0.45} \tag{6}$$

where V_d is the dimensionless velocity $\left(V_d = U_t\left(4\mu_L g/3\rho_L\right)^{-1/3}\right)$ and D_d is the dimensionless diameter $\left(D_d = d_{eq}\left(\mu_L/\rho_L\right)^{-2/3}\left(3/4g\right)^{-1/3}\right)$. Figure (4) shows a comparison between the present results and Eq. (6). The results are very close to the calculated values by Vecer et al. [61] correlation but its dependence on diameter is less severe. Although the range of Reynolds number in Vecer et al. [61] study covers the one in the present work, but it was provided for free bubble, not for a bubble rising through wall-bounded flow. Moreover, it is demonstrated that terminal velocity is directly proportional to fluid type [62]. Therefore, a same correlation was obtained for the present experiments by curve fitting method as follows:

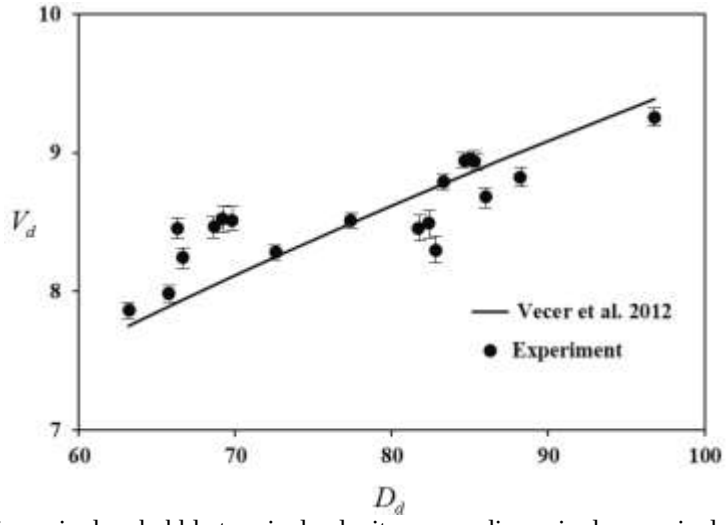

Figure 4 Dimensionless bubble terminal velocity versus dimensionless equivalent diameter; a comparison with Vecer et al. correlation

$$V_d = 142.7 D_d^{0.277} \tag{7}$$

3.2 Drag coefficient

One of the important concepts in analyzing bubble behavior is to calculate the drag coefficient based on different dimensionless groups, Reynolds and Eötvös numbers, at several fluids. As mentioned before, the main features of this study are the high Reynolds number and wall-bounded flow. Here, first the effect of bubble diameter on drag coefficient was examined, then the relation between dimensionless numbers and drag coefficient was analyzed. Figure (6) shows the variation of the drag coefficient with equivalent diameter. According to Figure (6) the drag coefficient depends on equivalent diameter of bubble almost linearly.

Deng et al. [32] also observed this increase for toluene droplet in deionized water. They denoted that the toluene drag coefficient, unlike rigid sphere, firstly decreases by increasing diameter then start to increase at a specific diameter. However, for the diameter range of 2*mm* to 4*mm*, they estimated that the drag coefficient is blow 0.2, which is much lower than the estimated value in the present work. This significant difference can be attributed to fluid in these works. Moreover, in the present work, the presence of surfactant as well as the effect of wall were influenced the results. Arkhipov et al. [35] investigated drag coefficient in the presence of surfactants in different diameters ranging from 0.4*mm* to 7*mm*.

They demonstrated that for $\mathrm{Re} < 1$, drag coefficient decreases and for $\mathrm{Re} > 200$, the drag coefficient is approximately 0.8. Liu et al. [63] has estimated the drag coefficient for the Re>135 to be constant and equal to 1.227 in distilled water. Here, the drag coefficient is underestimated due to the difference in fluid type. Sun et al. [64] was one of the group researchers who focused on the effect of bubble size on drag coefficient. They concluded that other factors such as surface tension, density and viscosity (generally fluid type) were also influenced that effect.

Figure (7) shows the variation of the drag coefficient with the Reynolds number in the experiments. As mentioned before, the high Reynolds number is one of the key distinctions between the present study and other works that achieved by adding bio surfactant. As indicated in Figure (7), the drag coefficient is almost independent of Reynolds number.

Li et al. [6] experiments, which were done on formation of hydrate films on bubble surfaces in the Reynolds number ranged from 50 to 800, shown the drag coefficient firstly decreases and reaches a minimum value at Re=150, then increases.

According to their results for the range of 400 to 800, the calculated drag coefficient is approximately constant. Similar trend was also indicated by Vecer et al. [61] for a fluid containing surfactant while neglecting the effect of surface tension. For the mentioned range of Re, they predicted that it various from 1 to 2, depend on the type of fluid and added surfactant and neglecting the effect of surface tension. Compared with the present study, it can be concluded that within the wall-bounded flow, the effect of surface tension is negligible. The results of Tagawa et al. [34] for a diameter of 1.5 *mm* show that in the range of Reynolds 300 to 900, the drag coefficient is independent on the Reynolds number. Also, Sun et al. [64] demonstrate that for $\mathrm{Re} > 100$, drag coefficient gradually reaches a constant value of 0.95. However, for $\mathrm{Re} < 300$, the drag coefficient depends on the Reynolds number [5, 34, 65]. Generally, considering the range of Reynolds and being wall-bounded flow, in this work, the independence of drag coefficient to Reynolds is the expected result. Moreover, the type of fluid and surfactant determines the value of drag coefficient (approximately).

Table (3) shows some typical correlations for drag coefficient prediction and their percentage error in estimating the present results. The lowest error in estimating the drag coefficient is related to Liu et al. [63] correlation. Although the dependency to all dimensionless numbers has been considered in this correlation, but its use is not recommended due to the complexity of the relation and the low effect of Reynolds number compared to Eötvös effect ($C_D \propto Re^{0.089} Eo^{0.951}$). Moreover, the difference in Weber numbers in the present experiments is not

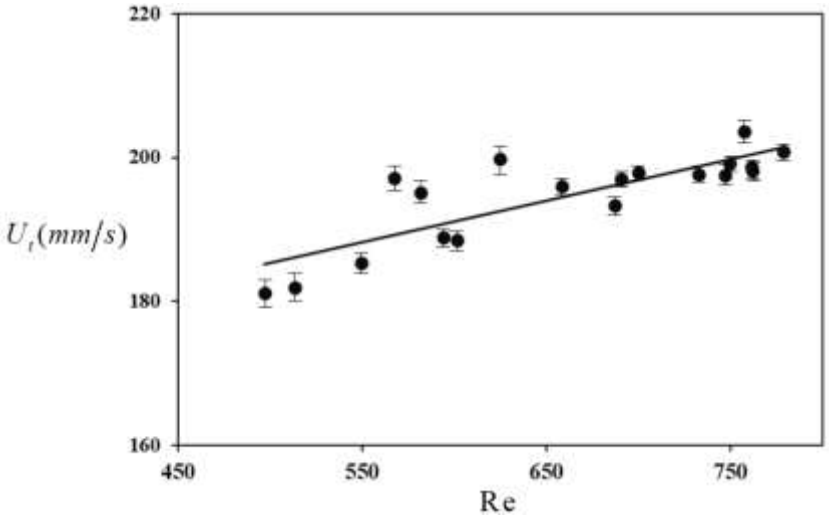

Figure 5 Bubble rising velocity versus Reynolds number

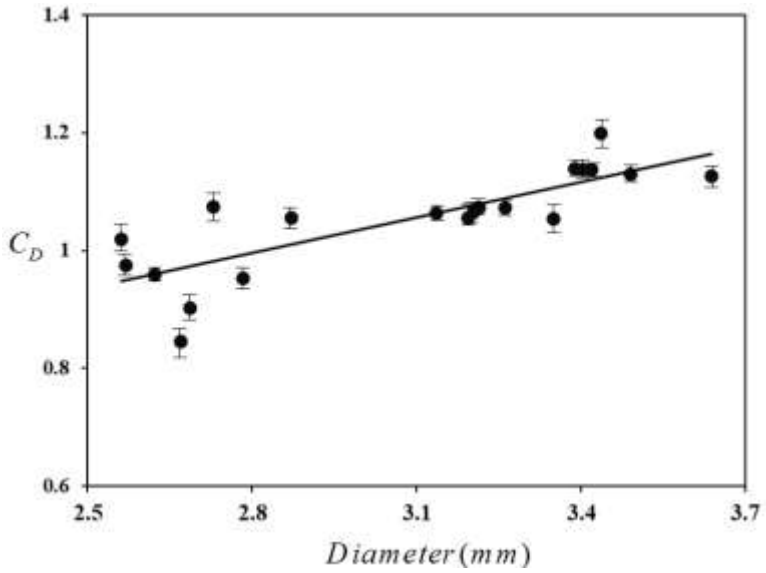

Figure 6 Effect of bubble diameter on drag coefficient

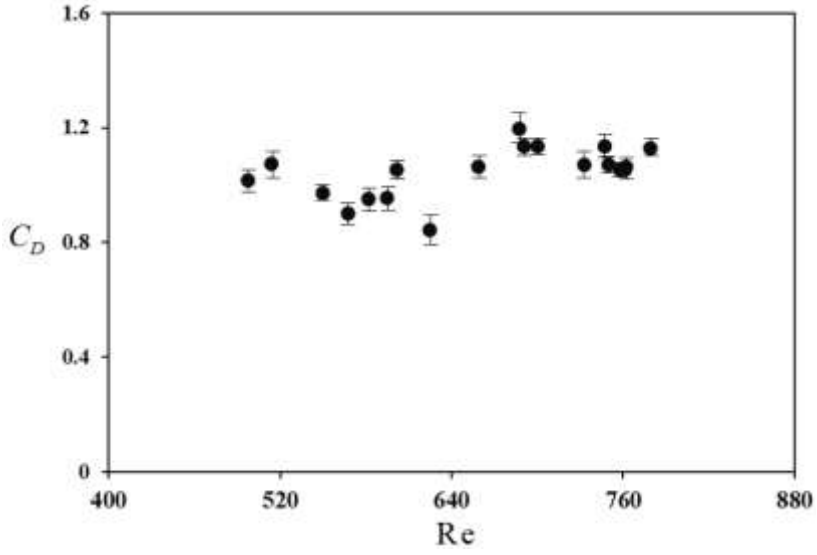

Figure 7 Drag coefficient variation with Reynolds number

so great (refer to Table 2). On the other words, due to the change of surface tension, the equivalent diameter and terminal velocity vary in such a way that the Weber number is almost constant.

According to the previous studies and the reported errors to determine bubble drag coefficient, the Eötvös number is more recommended than the Reynolds number. For example, Ishii and Chawla [67] for the first time, represent that for $Re<10^4$, the drag coefficient is related the Eötvös number and its relation to Re and We numbers was not significant. Zhang et al. [14] also provided a same correlation with different power and coefficient. This discrepancy is due to the different fluids used. Furthermore, similar findings was also presented by Kurimoto et al. [70] for glycerol–water solutions. Recently, Karimi et al. [47]presented two equations to calculate drag coefficient in rhamnolipid solutions. Figure (8) shows the dependence of the drag coefficient on Eötvös number in the present work and compare with the mentioned correlations. As it is shown, the drag coefficient increase by increasing Eötvös number.

It can be seen that none of the pervious correlations can fit all the experimental data very well. Therefore, it is recommended to provide a new correlation to determine bubble drag coefficient rising in rhamnolipid-contaminated liquid that is surrounded by column walls. Consequently, two correlations present to predict drag coefficient. The relations determined by curve fitting method are:

$$C_D = 0.86Eo^{0.174}$$
$$C_D = 1.09\text{-}0.22\exp\left(-0.5\left(\frac{Eo-2.5}{0.15}\right)^2\right)^2 \quad (9)$$

Table 3 Typical correlations for drag coefficient prediction

References	Expression	Application	Percentage error in estimating the present results
[66]	$C_D=\frac{24(1+0.15\mathrm{Re}^{0.687})}{\mathrm{Re}}$	$\mathrm{Re}<1000$	54.98%
[67]	$C_D=\frac{2}{3}E_O^{0.5}$	$\mathrm{Re}<10^4$	15.20%
[68]	$C_D=\frac{24}{\mathrm{Re}}(1+0.15\mathrm{Re}^{0.687})+\left(\frac{0.413}{1+16300\mathrm{Re}^{-1.09}}\right)$	$\mathrm{Re}<2\times10^5$	52.20%
[69]	$C_D=\frac{49.9}{\mathrm{Re}}(1-\frac{2.21}{\mathrm{Re}^{0.5}})1.17\times10^{-8}\mathrm{Re}^{2.615}$	$80<\mathrm{Re}<1530$	98.60%
[15]	$C_D=\frac{8}{3}\frac{E_O}{E_O+4}$	$0.01<\mathrm{Re}<100$ glycerol–water Triton X-100 as surfactant	14.89%
[14]	$C_D=0.579E_O^{0.216}$	$6500<\mathrm{Re}<9500$ metal liquid	29.21%
[63]	$C_D=\frac{24}{\mathrm{Re}}(1+0.15\mathrm{Re}^{0.687})\frac{\mathrm{Re}^{0.402}E_O^{0.915}We^{-0.381}}{e^{2.412}}$	$\mathrm{Re}<1000$ glycerol	9%
[63]	$C_D=1.227$	$135<\mathrm{Re}$ Distilled water	17.41%
[47]	$C_D=1.02E_O^{0.15}$ $C_D=\frac{1.41Eo}{Eo+0.57}$	$600<\mathrm{Re}<800$ rhamnolipid	13.59% 11.65%

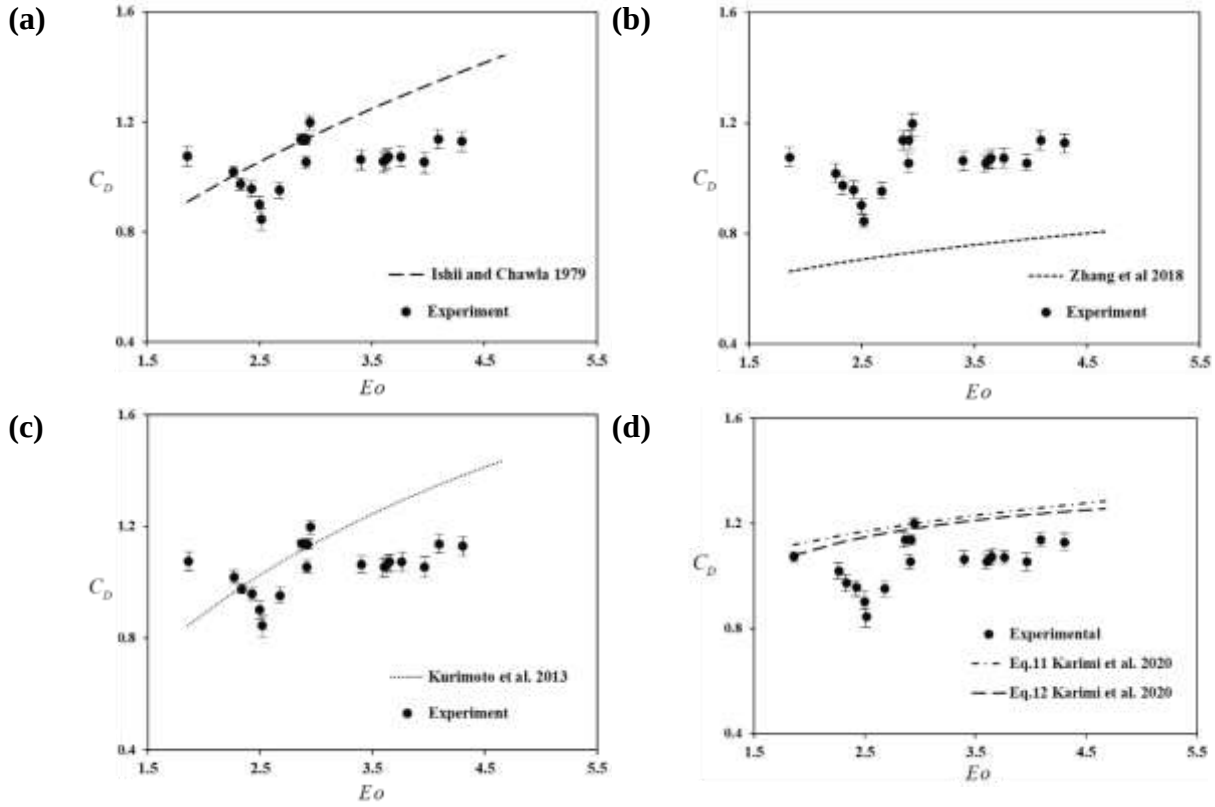

Figure 8 Measured drag coefficient versus Eo; compare with provided correlations: a) Ishii &Chawla, b) Zhang et al., c) Kurimoto et al., d) Karimi et al. correlations

The average error between experimental data and the ones quantified by Eqs. (8) and (9) are 4.44% and 3.26%, respectively, which indicated that they have a relatively good precision to predict the results.

4 Conclusion

In the present work, the behavior of a single bubble in a contaminated fluid was investigated through a wall-bounded flow. The main objective of this work was to evaluate bubble drag coefficient and terminal velocity at high Reynolds numbers experimentally. The results showed that the terminal velocity was approximately linearly dependent to bubble diameter. Accordingly, to show the dependency two correlations were provided both dimensionally and non-dimensionally with the average error of 3.35% and 1.97%, respectively. Moreover, the results of wall-bounded flow indicated that velocity and Reynolds number are related to each other. However, the resulted drag coefficient was independent to Reynolds number and changed by bubble diameter and Eötvös number. The conclusion was validated by comparing with previous studies. Finally, two convenient modified correlations were also provided to estimate the drag coefficient of a bubble rising at high Reynolds number in wall-bounded flow. The correlations were considered the relation between drag coefficient and Eötvös number. Average errors of these equations were 4.44% and 3.26%.

References

[1] Silva, M.,Campos, J., and Araújo, J., "General Correlations for Gas-liquid Mass Transfer in Laminar Slug Flow", International Communications in Heat and Mass Transfer, Vol. 120, pp. 104998, (2021).

[2] Yao, C., Ma, H., Zhao, Q., Liu, Y., Zhao, Y., and Chen, G., "Mass Transfer in Liquid-liquid Taylor Flow in a Microchannel: Local Concentration Distribution, Mass Transfer Regime and the Effect of Fluid Viscosity", Chemical Engineering Science, Vol. 223, pp. 115734, (2020).

[3] Fayzi, P., Bastani, D., and Lotfi, M., "A Note on the Synergistic Effect of Surfactants and Nanoparticles on Rising Bubble Hydrodynamics", Chemical Engineering and Processing-Process Intensification, Vol. 155, pp. 108068, (2020).

[4] Fayzi, P., Bastani, D., Lotfi, M., and Miller, R., "Influence of Surface-Modified Nanoparticles on the Hydrodynamics of Rising Bubbles", Chemical Engineering & Technology, Vol. 44, pp. 513-520, (2021).

[5] Hayashi, K.,and Tomiyama, A., "Effects of Numerical Treatment of Viscous and Surface Tension Forces on Predicted Motion of Interface", The Journal of Computational Multiphase Flows, Vol. 6, pp. 111-126, (2014).

[6] Li, H., Liu, Z., Chen, J., Sun, B., Guo, Y., and He, H., "Correlation of Aspect Ratio and Drag Coefficient for Hydrate-film-covered Methane Bubbles in Water", Experimental Thermal and Fluid Science, Vol. 88, pp. 554-565, (2017).

[7] Bora, M., Behera, S.K., and Deb, P., "Dynamic Coalescence and Implosion of Internal Microbubbles in Immobile Droplet", In: editor.^editors. AIP Conference Proceedings, ed.: AIP Publishing LLC. pp. 030014, (2020).

[8] Kim, S., Oshima, N., Murai, Y., and Park, H.J., "Numerical Investigation of a Single Intermediate-sized Bubble in Horizontal Turbulent Channel Flow", Journal of Fluid Science and Technology, Vol. 15, pp. JFST0020-JFST0020, (2020).

[9] Vitasari, D., Cox, S., Grassia, P., and Rosario, R., "Effect of Surfactant Redistribution on the Flow and Stability of Foam Films", Proceedings of the Royal Society A, Vol. 476, pp. 20190637, (2020).

[10] Moore, D., "The Boundary Layer on a Spherical Gas Bubble", Journal of Fluid Mechanics, Vol. 16, pp. 161-176, (1963).

[11] Lehrer, I.H., "A Rational Terminal Velocity Equation for Bubbles and Drops at Intermediate and High Reynolds Numbers", Journal of Chemical Engineering of Japan, Vol. 9, pp. 237-240, (1976).

[12] Almatroushi, E., and Borhan, A., "Surfactant Effect on the Buoyancy-Driven Motion of Bubbles and Drops in a Tube", Annals of the New York Academy of Sciences, Vol. 1027, pp. 330-341, (2004).

[13] Liu, L., Yan, H., Zhao, G., and Zhuang, J., "Experimental Studies on the Terminal Velocity of Air Bubbles in Water and Glycerol Aqueous Solution", Experimental Thermal and Fluid Science, Vol. 78, pp. 254-265, (2016).

[14] Zhang, C., Zhou, D., Sa, R., and Wu, Q., "Investigation of Single Bubble Rising Velocity in LBE by Transparent Liquids Similarity Experiments", Progress in Nuclear Energy, Vol. 108, pp. 204-213, (2018).

[15] Kurimoto, R., Hayashi, K., and Tomiyama, A., "Terminal Velocities of Clean and Fully-contaminated Drops in Vertical Pipes", International Journal of Multiphase Flow, Vol. 49, pp. 8-23, (2013).

[16] Batchvarov, A., Kahouadji, L., Magnini, M., Constante-Amores, C.R., Craster, R.V., Shin, S., Chergui, J., Juric, D., and Matar, O.K., "Effect of Surfactant on Elongated Bubbles in Capillary Tubes at High Reynolds Number", Phys Rev Fluids, Vol. 5, pp. 093605, (2020).

[17] Barbosa, C., Legendre, D., and Zenit, R., "Sliding Motion of a Bubble Against an Inclined Wall from Moderate to High Bubble Reynolds Number", Physical Review Fluids, Vol. 4, pp. 043602, (2019).

[18] Garnier, C., Lance, M., and Marié, J., "Measurement of Local Flow Characteristics in Buoyancy-driven Bubbly Flow at High Void Fraction", Experimental Thermal and Fluid Science, Vol. 26, pp. 811-815, (2002).

[19] Karimi, S., Shafiee, M., Abiri, A., and Ghadam, F., "The Drag Coefficient Prediction of a Rising Bubble through a Non-Newtonian Fluid", Amirkabir Journal of Mechanical Engineering, Vol. 52, No. 4, pp. 71-80, (2019).

[20] Ahmadpour, A., Amani, E., and Esmaili, M., "Numerical Simulation of Shear Thinning Slug Flows: the Effect of Viscosity Variation on the Shape of Taylor Bubbles and Wall Shear Stress", Journal of the Brazilian Society of Mechanical Sciences and Engineering, Vol. 41, pp. 48, (2019).

[21] Bozzano, G.,and Dente, M., "Shape and Terminal Velocity of Single Bubble Motion: a Novel Approach", Computers & Chemical Engineering, Vol. 25, pp. 571-576, (2001).

[22] Riboux, G., Risso, F., and Legendre, D., "Experimental Characterization of the Agitation Generated by Bubbles Rising at High Reynolds Number", Journal of Fluid Mechanics, Vol. 643, pp. 509, (2010).

[23] Yan, X., Jia, Y., Wang, L., and Cao, Y., "Drag Coefficient Fluctuation Prediction of a Single Bubble Rising in Water", Chemical Engineering Journal, Vol. 316, pp. 553-562, (2017).

[24] Tihon, J., and Ezeji, K., "Velocity of a Large Bubble Rising in a Stagnant Liquid Inside an Inclined Rectangular Channel", Physics of Fluids, Vol. 31, pp. 113301, (2019).

[25] Li, M., and Hu, L., "Experimental Investigation of the Behaviors of Highly Deformed Bubbles Produced by Coaxial Coalescence", Experimental Thermal and Fluid Science, Vol. 117, pp. 110114, (2020).

[26] Pietrasanta, L., Mameli, M., Mangini, D., Georgoulas, A., Michè, N., Filippeschi, S., and Marengo, M., "Developing Flow Pattern Maps for Accelerated Two-phase Capillary Flows", Experimental Thermal and Fluid Science, Vol. 112, pp. 109981, (2020).

[27] Kelbaliyev, G., and Ceylan, K., "Development of New Empirical Equations for Estimation of Drag Coefficient, Shape Deformation, and Rising Velocity of Gas Bubbles or Liquid Drops", Chemical Engineering Communications, Vol. 194, pp. 1623-1637, (2007).

[28] Baltussen, M., Kuipers, J., and Deen, N., "Direct Numerical Simulation of Effective Drag in Dense gas–liquid–solid Three-phase Flows", Chemical Engineering Science, Vol. 158, pp. 561-568, (2017).

[29] Chung, B., Cohrs, M., Ernst, W., Galdi, G.,and Vaidya, A., "Wake–cylinder Interactions of a Hinged Cylinder at Low and Intermediate Reynolds Numbers", Archive of Applied Mechanics, Vol. 86, pp. 627-641, (2016).

[30] Wolf, A., Rauh, C., and Delgado, A., "Dynamics and Long-time Behavior of a Small Bubble in Viscous Liquids with Applications to Food Rheology", Archive of Applied Mechanics, Vol. 86, pp. 979-1002, (2016).

[31] Chen, Q., Liu, Y., Wu, Q., Wang, Y., Liu, T., and Wang, G., "Global Cavitation Patterns and Corresponding Hydrodynamics of the Hydrofoil with Leading Edge Roughness", Acta Mechanica Sinica, Vol. 36, pp. 1202-1214, (2020).

[32] Deng, C., Huang, W., Wang, H., Cheng, S., He, X., and Xu, B., "Preparation of Micron-Sized Droplets and their Hydrodynamic Behavior in Quiescent Water", Brazilian Journal of Chemical Engineering, Vol. 35, pp. 709-720, (2018).

[33] Hayashi, K.,and Tomiyama, A., "Effects of Surfactant on Lift Coefficients of Bubbles in Linear Shear Flows", International Journal of Multiphase Flow, Vol. 99, pp. 86-93, (2018).

[34] Tagawa, Y., Takagi, S., and Matsumoto, Y., "Surfactant Effect on Path Instability of a Rising Bubble", Journal of Fluid Mechanics, Vol. 738, pp. 124-142, (2014).

[35] Arkhipov, V., Vasenin, I., and Usanina, A., "Dynamics of Bubble Rising in the Presence of Surfactants", Fluid Dynamics, Vol. 51, pp. 266-274, (2016).

[36] Li, X., Jiang, M., Huang, Z., and Zhou, Q., "Effect of Particle Orientation on the Drag Force in Random Arrays of Oblate Ellipsoids in Low-Reynolds-number Flows", AICHE Journal, Vol. 67, pp. e17040, (2021).

[37] Chen, L., and Dong, Y., "Numerical Investigation on Fluid Forces of Piggyback Circular Cylinders in Tandem Arrangement at Low Reynolds Numbers", Acta Mechanica Sinica, Vol. pp. 1-14, (2021).

[38] Ganguli, S., and Lele, S.K., "Drag of a Heated Sphere at Low Reynolds Numbers in the Absence of Buoyancy", Journal of Fluid Mechanics, Vol. 869, pp. 264-291, (2019).

[39] Tomiyama, A., Celata, G., Hosokawa, S., and Yoshida, S., "Terminal Velocity of Single Bubbles in Surface Tension Force Dominant Regime", International Journal of Multiphase Flow, Vol. 28, pp. 1497-1519, (2002).

[40] Hasadi, Y.E., and Padding, J., "On the Existence of Logarithmic Terms in the Drag Coefficient and Nusselt Number of a Single Sphere at High Reynolds Numbers", arXiv preprint arXiv:200710214, Vol. pp. (2020).

[41] Feng, J., Li, X., Bao, Y., Cai, Z., Gao, Z., "Coalescence and Conjunction of Two In-line Bubbles at Low Reynolds Numbers", Chemical Engineering Science, Vol. 141, pp. 261-270, (2016).

[42] Genç, M.S., Karasu, İ., and Açıkel, H.H., "An Experimental Study on Aerodynamics of NACA2415 Aerofoil at Low Re Numbers", Experimental Thermal and Fluid Science, Vol. 39, pp. 252-264, (2012).

[43] Guet, S., Ooms, G., and Oliemans, R., "Influence of Bubble Size on the Transition from Low-Re Bubbly Flow to Slug Flow in a Vertical Pipe", Experimental Thermal and Fluid Science, Vol. 26, pp. 635-641, (2002).

[44] Li, S. b., Fan, J. g., Li, R. d., and Wang, L., "Effect of Surfactants on Hydrodynamics Characteristics of Bubble in Shear Thinning Fluids at Low Reynolds Number", Journal of Central South University, Vol. 25, pp. 805-811, (2018).

[45] Massoud, E., Xiao, Q., El-Gamal, H., and Teamah, M., "Numerical Study of an Individual Taylor Bubble Rising through Stagnant Liquids under Laminar Flow Regime", Ocean Engineering, Vol. 162, pp. 117-137, (2018).

[46] Zhou, Y., Zhao, C., and Bo, H., "Analyses and Modified Models for Bubble Shape and Drag Coefficient Covering a Wide Range of Working Conditions", International Journal of Multiphase Flow, Vol. 127, pp. 103265, (2020).

[47] Karimi, S., Shafiee, M., Ghadam, F., Abiri, A., and Abbasi, H., "Experimental Study on Drag Coefficient of a Rising Bubble in the Presence of Rhamnolipid as a Biosurfactant", Journal of Dispersion Science and Technology, Vol. pp. (2020). DOI 10.1080/01932691.2019.1711109,

[48] Shi, P., Rzehak, R., Lucas, D., and Magnaudet, J., "Hydrodynamic Forces on a Clean Spherical Bubble Translating in a Wall-bounded Linear Shear Flow", Physical Review Fluids, Vol. 5, pp. 073601, (2020).

[49] Ekanayake, N.I., Berry, J.D., Stickland, A.D., Dunstan, D.E., Muir, I.L., Dower, S.K., and Harvie, D.J., "Lift and Drag Forces Acting on a Particle Moving with Zero Slip in a Linear Shear Flow Near a Wall", Journal of Fluid Mechanics, Vol. 904, pp. (2020).

[50] Chhabra, R.P., "*Bubbles, Drops, and Particles in Non-Newtonian Fluids*", ed.: CRC Press,(2006).

[51] Clift, R., Grace, J.R., and Weber, M.E., "Bubbles, Drops, and Particles", ed.: Courier Corporation,(2005).

[52] Unnikrishnan, A., and Chhabra, R., "An Experimental Study of Motion of Cylinders in Newtonian Fluids: Wall Effects and Drag Coefficient", The Canadian Journal of Chemical Engineering, Vol. 69, pp. 729-735, (1991).

[53] Fayzi, P., Bastani, D., Lotfi, M., and Ghamangiz Khararoodi, M., "The Effects of Bubble Detachment Shape on Rising Bubble Hydrodynamics", Scientia Iranica, Vol. 26, pp. 1546-1554, (2019).

[54] Zheng, K., Li, C., Yan, X., Zhang, H., and Wang, L., "Prediction of Bubble Terminal Velocity in Surfactant Aqueous Solutions", The Canadian Journal of Chemical Engineering, Vol. 98, pp. 607-615, (2019).

[55] Bird, R.B., Stewart, W.E., and Lightfoot, E.N., "*Transport Phenomena*", ed.: John Wiley & Sons, (2007).

[56] Abbasi, H., Hamedi, M.M., Lotfabad, T.B., Zahiri, H.S., Sharafi, H., Masoomi, F., Moosavi-Movahedi, A.A., Ortiz, A., Amanlou, M., and Noghabi, K.A., "Biosurfactant-producing Bacterium, Pseudomonas Aeruginosa MA01 Isolated from Spoiled Apples: Physicochemical and Structural Characteristics of Isolated Biosurfactant", Journal of Bioscience and Bioengineering, Vol. 113, pp. 211-219, (2012).

[57] Mahmoudi, S., Hashemi Shahraki, B., and Aghajani, M., "Experimental and Theoretical Investigation of CO_2 and Air Bubble Rising Velocity through Kerosene and Distilled Water in Bubble Column", Journal of Dispersion Science and Technology, Vol. 40, pp. 33-42, (2019).

[58] Ziqi, C., Yuyun, B., and Zhengming, G., "Hydrodynamic Behavior of a Single Bubble Rising in Viscous Liquids", Chinese Journal of Chemical Engineering, Vol. 18, pp. 923-930, (2010).

[59] Harmathy, T.Z., "Velocity of Large Drops and Bubbles in Media of Infinite or Restricted Extent", Aiche J, Vol. 6, pp. 281-288, (1960).

[60] Davies, R., and Taylor, G.I., "The Mechanics of Large Bubbles Rising through Extended Liquids and through Liquids in Tubes", Proceedings of the Royal Society of London Series A Mathematical and Physical Sciences, Vol. 200, pp. 375-390, (1950).

[61] Vecer, M.,Lestinsky, P.,Wichterle, K., and Ruzicka, M., "On Bubble Rising in Countercurrent Flow", International Journal of Chemical Reactor Engineering, Vol. 10, pp. 1-21, (2012).

[62] Mendelson, H.D., "The Prediction of Bubble Terminal Velocities from Wave Theory", AICHE Journal, Vol. 13, pp. 250-253, (1967).

[63] Liu, N.,Yang, Y.,Wang, J., Ju, B., Brantson, E.T., Tian, Y., Dong, Y., and Mahlalela, B., "Experimental Investigations of Single Bubble Rising in Static Newtonian Fluids as a Function of Temperature Using a Modified Drag Coefficient", Natural Resources Research, Vol. 29, pp. 2209–2226, (2020).

[64] Sun, B.,Guo, Y.,Wang, Z.,Yang, X.,Gong, P.,Wang, J., and Wang, N., "Experimental Study on the Drag Coefficient of Single Bubbles Rising in Static non-Newtonian Fluids in Wellbore", Journal of Natural Gas Science and Engineering, Vol. 26, pp. 867-872, (2015).

[65] Arkhipov, V.A.,Vasenin, I.,Tkachenko, A., and Usanina, A., "Unsteady Rise of a Bubble in a Viscous Fluid at Small Reynolds Numbers", Fluid Dynamics, Vol. 50, pp. 79-86, (2015).

[66] Schiller, L., and Naumann, Z., "A Drag Coefficient Correlation", Z Ver Deutsch Ing, Vol. 77, pp. 318-320, (1935).

[67] Ishii, M., and Chawla, T., "Local Drag Laws in Dispersed Two-phase Flow", Nasa Sti/Recon Technical Report N, Vol. 80, pp. 79-105, (1979).

[68] Turton, R., and Levenspiel, O., "A Short Note on the Drag Correlation for Spheres", Powder technology, Vol. 47, pp. 83-86, (1986).

[69] Rodi, W., and Fueyo, N., "Engineering Turbulence Modelling and Experiments 5 Proceedings of the 5th International Symposium on Engineering Turbulence Modelling and Measurements", Mallorca, Spain, 16–18 September, (2002).

[70] Kurimoto, R.,Hayashi, K., and Tomiyama, A., "Terminal Velocities of Clean and Fully-Contaminated Drops in Vertical Pipes", International Journal of Multiphase Flow, Vol. 49, pp. 8-23, (2013).

Nomenclature

A_b	Area of bubble (mm^2)
Bo	Bond number
C_D	Drag coefficient
CMC	Critical micelle concentration
D_d	dimensionless diameter
d_{eq}	Equivalent diameter (*mm*)
Eo	Eötvös number
g	Gravitational acceleration (m/s^2)
Mo	Morton number
Re	Reynolds number
V_d	Dimensionless velocity
U_t	Terminal velocity(*mm/s*)

Greek Symbols

μ_l	Liquid viscosity (*cp*)
ρ_g	Densities of the gas (kg/m^3)
ρ_l	Densities of the liquid (kg/m^3)
σ	Surface tension between fluid and bubble (*N/m*)